Article

Time-bin entangled qubits for quantum communication created by femtosecond pulses

MARCIKIC, Ivan, *et al*.

Abstract

We create pairs of non-degenerate time-bin entangled photons at telecom wavelengths with ultra-short pump pulses. Entanglement is shown by performing Bell kind tests of the Franson type with visibilities of up to 91%. As time-bin entanglement can easily be protected from decoherence as encountered in optical fibers, this experiment opens the road for complex quantum communication protocols over long distances. We also investigate the creation of more than one photon pair in a laser pulse and present a simple tool to quantify the probability of such events to happen.

Reference

MARCIKIC, Ivan, *et al*. Time-bin entangled qubits for quantum communication created by femtosecond pulses. *Physical review, A, Atomic, molecular, and optical physics*, 2002, vol. 66, no. 6

DOI : 10.1103/PhysRevA.66.062308

Time-bin entangled qubits for quantum communication created by femtosecond pulses

I. Marcikic,[1] H. de Riedmatten,[1] W. Tittel,[1,2] V. Scarani,[1] H. Zbinden,[1] and N. Gisin[1]
[1]*Group of Applied Physics-Optique, University of Geneva, CH-1211, Geneva 4, Switzerland*
[2]*Danish Quantum Optics Center, Institute for Physics and Astronomy, University of Aarhus, Aarhus, Denmark*
(Received 10 June 2002; published 10 December 2002)

We create pairs of nondegenerate time-bin entangled photons at telecom wavelengths with ultrashort pump pulses. Entanglement is shown by performing Bell kind tests of the Franson type with visibilities of up to 91%. As time-bin entanglement can easily be protected from decoherence as encountered in optical fibers, this experiment opens the road for complex quantum communication protocols over long distances. We also investigate the creation of more than one photon pair in a laser pulse and present a simple tool to quantify the probability of such events to happen.

DOI: 10.1103/PhysRevA.66.062308 PACS number(s): 03.67.Hk

I. INTRODUCTION

Entanglement is one of the most important tools for the realization of complex quantum communication protocols, like quantum teleportation or entanglement swapping, and due to their ability to be transported in optical fibers, photons are the best candidates for long-distance applications [1]. Even though some of these protocols have already been experimentally realized [2–8], none of them was optimized for long-distance communication. Most of them used polarization entangled photon pairs in the visible range which, are subject to important attenuation and suffer from decoherence (depolarization) due to polarization mode dispersion (birefringence) in optical fibers. Energy-time entanglement or its discrete version, time-bin entanglement [9], are more robust for long-distance applications since they are not sensitive to polarization fluctuation in optical fibers, and chromatic dispersion can be passively compensated using linear optics [10]. Indeed, both types have been proven to be well suited for transmission over more than 10 km [11,12], and have already been used for quantum cryptography [13,14]. However these experiments did not rely on joint measurements of photons from different pairs where the emission time of each pair must be defined to much higher precision. For this purpose we built and tested a new source using femtosecond pump pulses. This is the first femtosecond source at telecommunication wavelengths, and the first femtosecond source employing time-bin entanglement. This will allow realization of teleportation and entanglement swapping over long distances.

Apart from ensuring good localization of the photon pairs, a femtosecond pulse engenders a significant probability of creating a pair per pulse due to the high energy contained in each pulse, an important requirement where two pairs have to be created at the same time. However when this probability becomes significant, the probability of creating unwanted multiple pairs becomes higher. Thus, the purity of entanglement will decrease, a phenomenon that is unwanted for almost all quantum communication protocols (Bell test, cryptography, teleportation, etc.). For instance, the photon pair visibility in a Bell-type test will strongly depend on the relation between the multiple pairs. They can be either independent or they can be described as multiphoton entanglement.

In the following, we first remind the reader of the basic principle of time-bin entanglement, and we explain how to test entanglement. We then describe the experimental setup we used and present the results. In addition, we experimentally verify the reduction of the visibility due to multiple-pair creation. Finally, we present a straightforward measurement of the probability to create a pair per pulse.

II. FEMTOSECOND TIME-BIN ENTANGLEMENT

A time-bin qubit is formed by a coherent superposition of amplitudes describing a photon to be in two time-bins separated by a time difference that is much larger than the coherence time of the photon. It is created by a short pulse (in our case a femtosecond pulse) passing through an unbalanced interferometer, referred to as the pump interferometer, with a relative phase φ between the two arms. The output state of the photon, after the pump interferometer, can be written as

$$|\Psi\rangle_p = \frac{1}{\sqrt{2}}(|1,0\rangle - e^{i\varphi}|0,1\rangle). \tag{1}$$

The state $|1,0\rangle$ ($|0,1\rangle$) corresponds to the case where one photon is in the first (second) time bin, i.e., has been transmitted by the short (long) arm of the interferometer. The time separation between time bins is thus defined by the optical path difference between the short and the long arms. Entangled time-bin qubits are created by passing a time-bin qubit through a nonlinear crystal where eventually twin photons can be created by spontaneous parametric down-conversion. The creation time is then given by the superposition of two values:

$$|\Phi\rangle = \frac{1}{\sqrt{2}}(|1,0\rangle_A|1,0\rangle_B - e^{i\varphi}|0,1\rangle_A|0,1\rangle_B). \tag{2}$$

The indexes A and B label the signal and idler photons that are separated and sent to Alice and Bob. Depending of the relative phase φ, two out of four Bell states can be created ($\Phi^{\pm}$). The two remaining Bell states ($\Psi^{\pm}$) can be created in principle with switches and delays after the crystal.

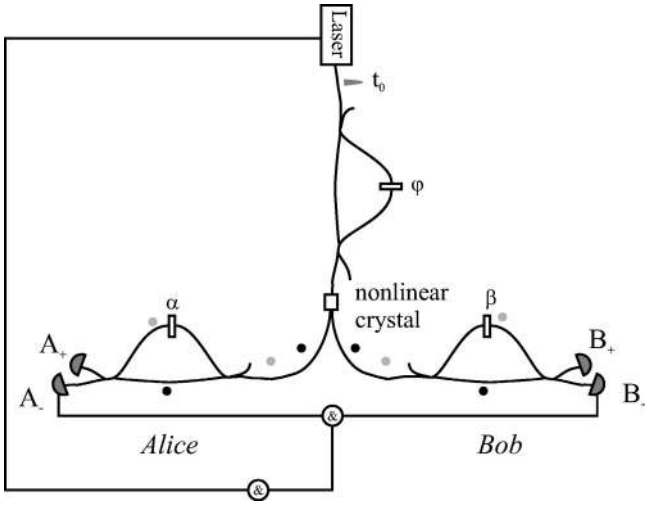

FIG. 1. Scheme of a Bell type experiment using time-bin entangled photons. Time-bin qubits are prepared by passing a femtosecond pulse through the pump interferometer. Eventually, a pair of entangled photons is created in the crystal. Alice and Bob analyze the photons using interferometers that are equally unbalanced with respect to the pump interferometer, thereby sending the amplitude in the first (gray) time bin through the long arm and the one in the second (black) time bin through the short arm and thus undoing the transformation of the pump interferometer (in 50% of the cases).

A. Bell test

To qualify the purity and degree of entanglement, we perform a Bell test (Franson type) [15]. One of the photons is sent to Alice and the other one to Bob (see Fig. 1).

To analyze the received qubit, Alice and Bob undo the initial transformation with an interferometer that has the same optical path length difference as the pump interferometer. For instance, the initial state $|1,0\rangle_A$ evolves as follows:

$$|1,0\rangle_A \mapsto \frac{1}{2}[\,|1,0,0\rangle_{A_-}|0,0,0\rangle_{A_+} - e^{i\alpha}|0,1,0\rangle_{A_-}|0,0,0\rangle_{A_+} + i|0,0,0\rangle_{A_-}|1,0,0\rangle_{A_+} + ie^{i\alpha}|0,0,0\rangle_{A_-}|0,1,0\rangle_{A_+}]. \tag{3}$$

The state $|n_0,n_1,n_2\rangle_{A+}$ corresponds to the case where n_0 photons are in the first time bin (passing zero times through the long arm of any interferometer), n_1 photons are in the second time bin (passing once through a long arm of any interferometer), n_2 photons are in the third time bin (passing through the long arms of two different interferometers). The index $A\pm$ ($B\pm$) represents Alice's (Bob's) detectors as depicted in Fig. 1. Taking into account similar evolution for three other states, Eq. (2) becomes

$$\begin{aligned}|\Psi\rangle = \frac{1}{4\sqrt{2}}[&(e^{i(\alpha+\beta)} - e^{i\varphi})|0,1,0\rangle_{A_-}|0,1,0\rangle_{B_-} \\ &- i(e^{i(\alpha+\beta)} + e^{i\varphi})|0,1,0\rangle_{A_-}|0,1,0\rangle_{B_+} \\ &- i(e^{i(\alpha+\beta)} + e^{i\varphi})|0,1,0\rangle_{A_+}|0,1,0\rangle_{B_-} \\ &- (e^{i(\alpha+\beta)} - e^{i\varphi})|0,1,0\rangle_{A_+}|0,1,0\rangle_{B_+} \\ &+ (24 \text{ other terms})].\end{aligned} \tag{4}$$

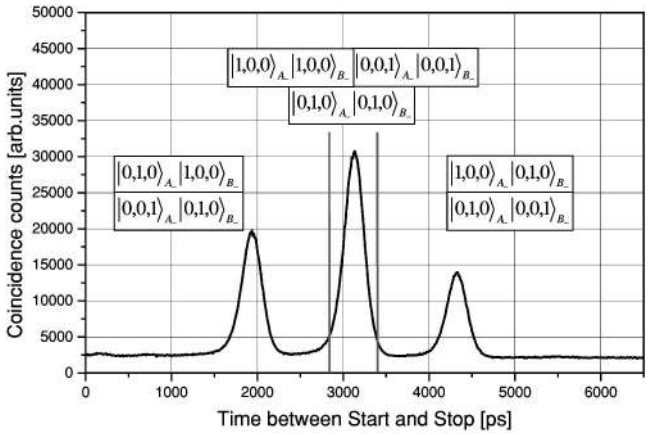

FIG. 2. Time histogram of the difference of arrival times between Alice and Bob's detector. The spacing between two peaks corresponds to the optical path difference in any interferometer.

In the following discussion, we are interested only in coincidences between A_- and B_- detectors (see Fig. 1). If we monitor the difference of arrival times of two entangled photons at Alice and Bob's side ($t_{A_-} - t_{B_-}$), with a time-to-amplitude converter (TAC), we distinguish three different peaks (see Fig. 2).

The two satellite peaks correspond to events that are well distinguishable $|0,1,0\rangle_{A_-}|1,0,0\rangle_{B_-}$ or $|0,0,1\rangle_{A-}|0,1,0\rangle_{B_-}$ for the left satellite peak and $|1,0,0\rangle_{A_-}|0,1,0\rangle_{B_-}$ or $|0,1,0\rangle_{A_-}|0,0,1\rangle_{B_-}$ for the right satellite peak. These peaks can be discarded by selecting a sufficiently small time window around the central peak. In the central peak, three events (due to Alice and Bob's photons taking the same path in the respective interferometers) are counted: $|1,0,0\rangle_{A_-}|1,0,0\rangle_{B_-}$, $|0,0,1\rangle_{A_-}|0,0,1\rangle_{B_-}$, and $|0,1,0\rangle_{A_-}|0,1,0\rangle_{B_-}$. The first (second) event corresponds to the case when the photons created in the first (second) time bin pass through the short (long) arm of Alice and Bob's interferometer. The third event corresponds either to the case where the photons created in the first time bin pass through the long arm of Alice (acquiring a relative phase α) and Bob's (acquiring a relative phase β) interferometer or to the case where the photons created in the second time bin (with a relative phase φ) pass through the short arm of Alice's and Bob's interferometer. The impossibility to distinguish, even in principle, via which path the photons have passed leads to interference. Knowing the emission time of the pump pulse, we can distinguish two out of three events ($|1,0,0\rangle_{A_-}|1,0,0\rangle_{B_-}$ and $|0,0,1\rangle_{A_-}|0,0,1\rangle_{B_-}$), thus the visibility as observed in the two-photon interference while changing the phase in one of the three interferometers is limited to 50%. To increase the visibility to 100%, we postselect the third event by making a threefold coincidence between the emission time of the pump photon, and Alice and Bob's detection (see Fig. 1). Thus the postselected state is

$$|\Psi\rangle_{postselected} = |0,1,0\rangle_{A_-}|0,1,0\rangle_{B_-}, \tag{5}$$

with the amplitude of probability to be detected being

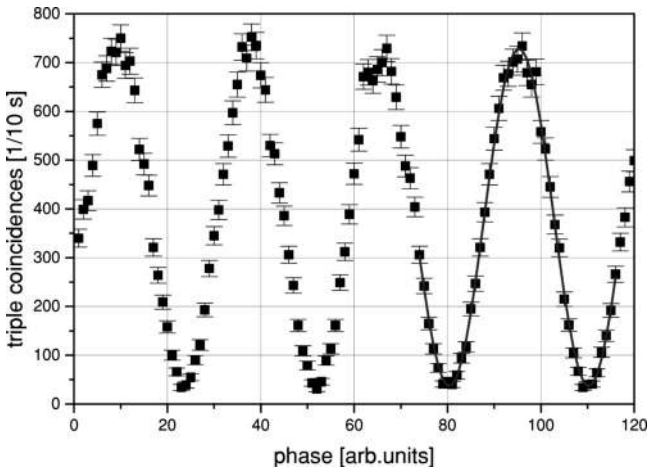

FIG. 3. Net interference fringes of the triple-coincidence detection of the postselected state [Eq. (5)].

$$A \simeq e^{i(\alpha+\beta-\varphi)} - 1.$$

Here φ, α, and β are the relative phases of the pump, Alice's and Bob's interferometer, respectively. The triple-coincidence counting rate is, thus, given by

$$R_c \sim 1 - V\cos(\alpha+\beta-\varphi), \tag{6}$$

where V is the visibility that can in principle reach the value of 1. We take it as the figure of merit to quantify the entanglement. Note that correlation described by such coincidence functions with a visibility higher than 70.7% cannot be described by local theories [16].

B. Experimental setup

A mode-locked Ti:sapphire laser (Coherent Mira 900) produces pulses at $\lambda_p = 710$ nm with 150-fs pulse width and 76-MHz repetition rate. To remove all unwanted infrared light, the light passes through a series of dichroic mirrors, reflecting only wavelengths centered around 710 nm. The superposition of discrete times is made by a bulk Michelson interferometer with a path-length difference of 1.2 ns [17]. The entangled nondegenerate collinear photons at 1310 and 1550 nm (telecom wavelengths) are created in a $KNbO_3$ type-I nonlinear crystal. The pump light is removed with a RG 1000 filter, the twin photons are collimated into an optical fiber and separated by a wavelength-division multiplexer (WDM). The analyzers are two Michelson fiber interferometers with Faraday rotator mirrors. The role of these mirrors is to compensate any difference of polarization transformation in the two arms of the interferometer [18,19]. The phase is tuned by varying the temperature of the interferometer.

At Alice's side, the photon counter at 1310 nm is a passively quenched germanium avlanche photodiode (APD), cooled with liquid nitrogen and working in reversed mode above the breakdown voltage (so-called Geiger mode). The quantum efficiency is around 10% for a dark count rate of 20 kHz. At Bob's side the photons at 1550 nm are detected by a indium gallium arsenide (InGaAs) APD, Peltier cooled to around $-50°$C. To obtain a good signal-to-noise ratio, these APDs have to be used in the so-called gated mode. They are then operational only during a short period (around 50 ns) when a photon is expected to arrive. Thus, the InGaAs APD is triggered by the Ge APD. Its quantum efficiency is around 30% for a dark count probability of $\sim 10^{-4}$/ns [20].

The twin photons, due to our phase-matching conditions, have a large spectral bandwidth of around 90 nm. To reduce the effect of chromatic dispersion in our interferometers, we limit the spectral width of the down-converted photons with an interference filter at Alice's side ($\Delta\lambda = 40$ nm) [21], and we use dispersion shifted fibers for Bob's interferometer. In addition, spectral filtering of the 1310-nm photons leads to a decrease of the count rate of the Ge detector, hence to a decrease of the trigger rate for the $In_xGa_{1-x}As$ APD which enables to operate them at a higher quantum efficiency.

C. Results of the measurement

Figure 3 shows the typical results of an interference curve. The visibility of the interference fringes, after subtraction of the noise, is $(91 \pm 0.8)\%$ (computed using a sinusoidal fit). This result shows that the created state is not far from a pure maximally entangled state, sufficiently entangled to be used in quantum communication protocols. Please note that only the net visibility is important in this context. Indeed, we have to subtract the accidental coincidences from the raw visibility since they are due to a combination of fiber losses, nonperfect quantum efficiency, and detector noise, and not to reduced entanglement. However, if we assume (in addition to Ref. [22]) that the accidental coincidences are measured in a fair way, our net visibility is high enough to violate the CHSH inequality [16] by more than 25 standard deviations.

Note that with this source, creating entangled photons with the same polarization and using time-bin entanglement, we did not have problems met by other groups creating polarization entangled photons with a femtosecond pulsed laser [23]. The quality of our entanglement is not degraded by the use of the long crystal ($l = 10$ mm) and large interference filters ($\Delta\lambda = 40$ nm).

III. MULTIPHOTON STATES

The above-mentioned results were obtained using a mean pump power of 24 mW. By increasing the pump power the probability of creating more than one pair per pulse increases too, thus the visibility of the two-photon interference fringes decreases. Although the pump power was chosen in order to get good visibilities, this effect is still present. Figure 4 shows the decrease of the visibility as a function of the pump power.

The decrease of the visibility can be understood with the following simple calculation that can be rederived using the full formalism of quantum optics [24]. The normalized detection rate is the sum of two mutually incoherent contributions: R_2, the detection rate associated to the production of one pair; and R_4, associated to the production of four pho-

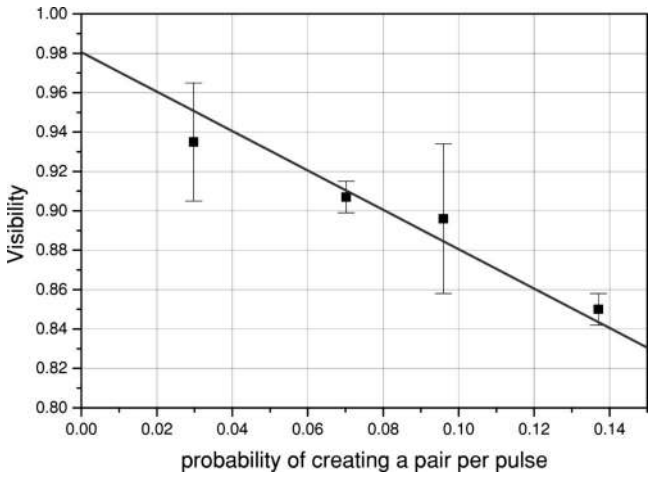

FIG. 4. Decrease of the visibility as function of the pump power. The solid line represents the theoretical predictions $V(P_{pair}) = V_{max} - P_{pair}$, the fit yielding $V_{max} = 98\%$.

tons. The two-photon contribution has 100% visibility, thence we can write

$$R_2 = P_{pair} \frac{1+\cos\theta}{2}, \tag{7}$$

where P_{pair} is the probability of creating one pair and $\theta = \alpha + \beta - \varphi$. We discuss the four-photon contribution supposing that the four-photon state is actually two independent pairs, which is not strictly true, but is a good guide for the intuition—moreover, the final result turns out to be independent of this assumption [24]. Thus we have two possible cases: when the two photons that are detected belong to the same pair, R_4 shows full interference; when they belong to different pairs, R_4 shows no interference at all. Each of the situations happens twice, because the two pairs may have been created either both in the same pulse, or one in each pulse. Thus

$$R_4 = P_{four\ photons}\left(2\frac{1+\cos\theta}{2} + 2\frac{1}{2}\right)$$

$$= 4P_{four\ photons}\frac{1+\frac{1}{2}\cos\theta}{2}. \tag{8}$$

Now assuming a Poissonian distribution for counting of independent events, the probability of creating four photons is $P_{four\ photons} = P_{pair}^2/2$. So finally

$$R_c = \frac{1}{2}[(P_{pair} + 2P_{pair}^2) + (P_{pair} + P_{pair}^2)\cos\theta], \tag{9}$$

whence the total visibility [defined in Eq. (6)] is $V = (1+P_{pair})/(1+2P_{pair}) \approx 1 - P_{pair}$, predicting a slope of -1, which is in excellent agreement with the results shown in Fig. 4.

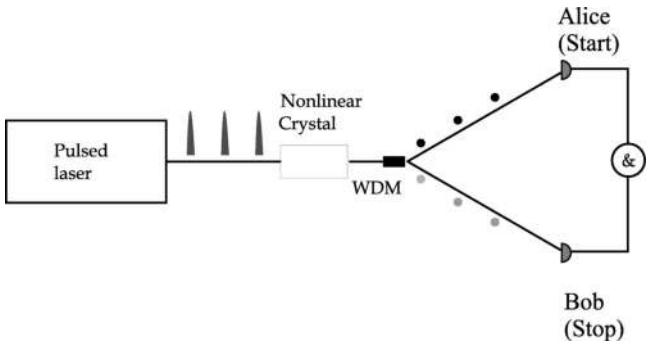

FIG. 5. Experimental setup for the measurement of the probability of creation of a pair per pulse.

IV. CHARACTERIZATION OF THE SOURCE

As we have seen in the last section, it is important to get a fast and reliable estimation of the probability of creating a pair per pulse. Usually this probability is computed from

$$P_{pair} = N(\text{singles})/t_A \eta_A f, \tag{10}$$

where P_{pair} is the probability of creating a pair per pulse, N(singles) is the number of photons detected by Alice, t_A characterizes coupling and transmission, η_A is the quantum efficiency of Alice's detector, and f is the laser frequency. In this case we have to estimate the values of t_A and η_A (the quantum efficiency can be measured but it is not a straightforward measurement).

We present in this section a new, easily visualized, and straightforward way of measuring this probability. The experimental setup is very simple:

A series of femtosecond pulses pass through a nonlinear crystal creating pairs of photons at 1310 and 1550 nm, which are separated with a WDM (see Fig. 5). Each of them is detected with the same detectors as in the previous experiment, and the difference of arrival times between Alice and Bob's photon is measured with a TAC.

If every created photon was detected, we would obtain only one main peak, but because of imperfect detector efficiency, coupling, and transmission losses, we observe the apparition of, what we call, side peaks (see Fig. 6). These side peaks have been observed in different contexts as well (for instance, Ref. [25]).

The right (left) side peak is due to events where the start at Alice's side is given by a photon created by a pulse, but where its twin is not detected at Bob's side. The stop is then given by another photon created by the following (preceding) pulse. By measuring the ratio between the main peak and the side peak we obtain directly the required probability:

$$P_{pair} = \frac{(\text{counts in the side peak})}{(\text{counts in the mainpeak})}. \tag{11}$$

This equation holds only for $t_B \eta_B \ll 1$. The theoretical development is presented in the Appendix.

Figure 7 depicts the pair creation rate, calculated from the ratio of side to main peak [Eq. (11)], as a function of the single count rate of the Ge detector. The solid line shows the

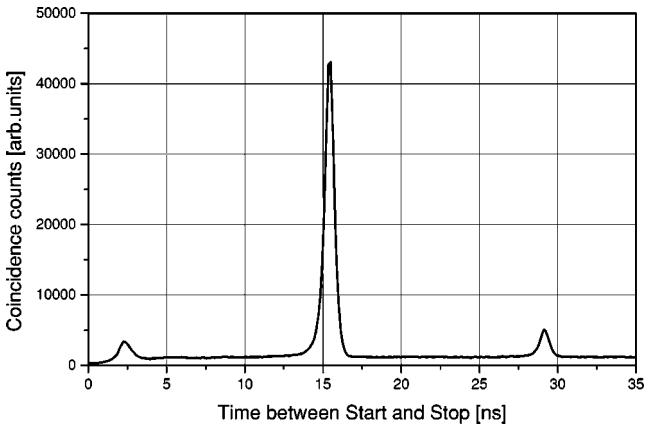

FIG. 6. Time histogram of the difference of arrival times between Alice's and Bob's detector. The spacing between two peaks is equal to the spacing between two laser pulses.

prediction based on Eq. (10) where we estimate $t_A = 30\%$ and $\eta_A = 9\%$ [26]. We see that both methods are in qualitative agreement, the deviation of the measured points from the solid line is due to the fact that in practice $t_A \eta_A$ vary.

Our method has two main advantages compared to the standard one [Eq. (10)]: It is easily visualized and it immediately gives a good indication as to whether the probability to have more than one pair is significant; Second, no estimation has to be done, the probability is computed only from measured values, and the uncertainty of P_{pair} is smaller than when using the method mentioned previously (see the Appendix).

V. CONCLUSION

In this paper we presented a different source for realization of complex quantum protocols over long distances. This new source is the first one creating time-bin entangled qubits at telecom wavelengths with ultrashort pulses. We characterized this source by performing Bell-type tests, obtaining net coincidence visibilities of up to $(91 \pm 0.8)\%$. We investigated its dependence on the probability to create a photon pair and found excellent agreement between experimental results and theoretical prediction. Finally, we presented a new and simple tool for measuring the probability of creating a pair per pulse.

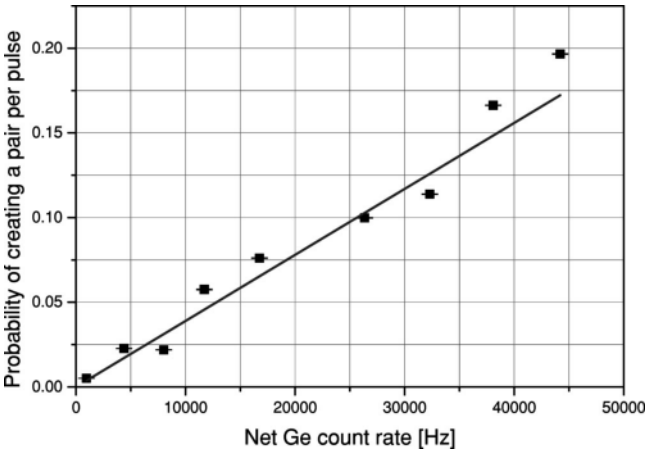

FIG. 7. Pair creation rate as a function of the single count rate of the 1310 nm photon detector (hence pump power). The points are values calculated from the ratio between side and main peaks, the solid line is a prediction based on Eq. (10) assuming that $t_A = 30\%$ and $\eta_A = 9\%$.

ACKNOWLEDGMENTS

This work was supported by the Swiss OFES in the frame of the European QuComm IST project and by the Swiss NCCR "Quantum Photonics." W.T. acknowledges financial support by ESF Program Quantum Information Theory and Quantum Computation (QIT).

APPENDIX

Figure 6 shows the histogram of the photon arrival time difference at Alice and Bob's detector. When there is a detection in the main peak, then start and stop are given by photons created by the same pump pulse. If N is the number of pairs created per pulse, then the probability of detecting a coincidence is given by

$$P_{\text{main peak}} = \sum_{N \geq 1}^{\infty} P(N|\text{start}) P(\text{stop}_0|N).$$

Here, $P(N|\text{start})$ is the probability of having N pairs, knowing that there was a start. $P(\text{stop}_0|N)$ is the probability of detecting a stop by one of the photons created by the *same* pulse as the one that gave the start.

The first term can be easily computed with Bayes' rule:

$$P(N|\text{start}) = \frac{P(N\&\text{start})}{P(\text{start})} = \frac{P(N)P(\text{start}|N)}{P(\text{start})},$$

where $P(N)$ is the probability that N pairs are emitted. If N pairs are created, the probability that the start is *not* given is $[1 - P(\Delta\lambda_A) t_A \eta_A]^N$, where $P(\Delta\lambda_X)$ describes the probability that a created photon passes through a possibly included interference filter—that is, $P(\Delta\lambda_X) = 1$ if there is no filter; as in the main text, t_X characterizes the coupling ratio and transmission, and η_X is the quantum efficiency of the detector. Therefore, the probability of having a start, knowing that N pairs were created, is given by

$$P(\text{start}|N) = 1 - (1 - P(\Delta\lambda_A) t_A \eta_A)^N.$$

Of course, $P(\text{start}) = \Sigma_{M=0}^{\infty} P(M) P(\text{start}|M)$, but this is a global factor that plays no role in what follows.

In the same way, we find

$$P(\text{stop}_0|N) = 1 - [1 - P(\Delta\lambda_B|\Delta\lambda_A) t_B \eta_B]^N,$$

where $P(\Delta\lambda_B|\Delta\lambda_A)$ is the probability that a photon at Bob's side passes through an interference filter knowing that its twin photon has already passed through an interference filter at Alice's side, thus $P(\Delta\lambda_B|\Delta\lambda_A) = 1$ when $\Delta\lambda_B \geqslant \Delta\lambda_A$ [21].

We assume that the spectrum of the created photons is centered at the maximum transmission of the interference filters.

The probability of detecting a coincidence in the right side peak is given by

$$P_{\text{side peak}} = \sum_{N \geqslant 1}^{\infty} P(N|\text{start})[1 - P(\text{stop}_0|N)]P(\text{stop}_1).$$

The first term represents, as before, the probability of having N pairs knowing that there was a start, the second is the probability not to detect a stop originating from the same pump pulse; $P(\text{stop}_1)$ is the probability that the stop is given by a photon created by the first pulse following the one which gave the start. Explicitly,

$$P(\text{stop}_1) = \sum_{M=0}^{\infty} P(M)[1 - (1 - P(\Delta\lambda_B)t_B\eta_B)^M];$$

note that here we have $P(\Delta\lambda_B)$ instead of $P(\Delta\lambda_B|\Delta\lambda_A)$, since we do not require that the twin photon has passed through the corresponding filter.

We now suppose that the mean number of pairs is much smaller than 1, so that $P(N>1)=0$ and $P(1)=P_{pair}$. From the equations above, we find the ratio between main and side peak to be

$$\frac{P_{\text{main peak}}}{P_{\text{side peak}}} = \frac{P(\Delta\lambda_B|\Delta\lambda_A)}{P_{pair}[1 - P(\Delta\lambda_B|\Delta\lambda_A)t_B\eta_B]P(\Delta\lambda_B)}.$$

If there is only one filter at Alice's side (as was in our Bell-type experiment) and $t_B\eta_B \ll 1$, we find Eq. (11) [$P(\Delta\lambda_B|\Delta\lambda_A)=1$ and $P(\Delta\lambda_B)=1$]. Thus, if one wants to measure the probability of creating a pair per pulse in a given spectral bandwidth, one has to filter both photons.

Finally, using this method, the uncertainty of P_{pair} is reduced compared to the standard method [Eq. (10)]. For instance, if we estimate $t_B=(30\pm 6)\%$ and $\eta_B=(30\pm 6)\%$, then the relative uncertainty of P_{pair} [calculated using Eq. (10)] is 30%, while it is only 3% using our method [Eq. (11)].

[1] W. Tittel and G. Weihs, Quantum Inf. Comput. **1**, 5 (2001).

[2] D. Bouwmeester, J.W. Pan, K. Mattle, M. Eibl, H. Weinfurter, and A. Zeilinger, Nature (London) **390**, 575 (1997).

[3] D. Boschi, S. Branca, F. De Martini, L. Hardy, and S. Popescu, Phys. Rev. Lett. **80**, 1121 (1998).

[4] A. Furusawa, J.L. Srensen, S.L. Braunstein, C.A. Fuchs, H.J. Kimble, and E.S. Polzik, Science **282**, 706 (1998).

[5] Y.-H. Kim, S.P. Kulik, and Y. Shih, Phys. Rev. Lett. **86**, 1370 (2001).

[6] E. Lombardi, F. Sciarrino, S. Popescu, and F. De Martini, Phys. Rev. Lett. **88**, 070402 (2002).

[7] J.-W. Pan, D. Bouwmeester, H. Weinfurter, and A. Zeilinger, Phys. Rev. Lett. **80**, 3891 (1998).

[8] T. Jennewein, G. Weihs, J.W. Pan, and A. Zeilinger, Phys. Rev. Lett. **88**, 017903 (2002).

[9] J. Brendel, N. Gisin, W. Tittel, and H. Zbinden, Phys. Rev. Lett. **82**, 2594 (1999).

[10] H. Zbinden, J. Brendel, N. Gisin, and W. Tittel, Phys. Rev. A **63**, 022111 (2001), and references therein.

[11] W. Tittel, J. Brendel, H. Zbinden, and N. Gisin, Phys. Rev. Lett. **81**, 3563 (1998).

[12] R.T. Thew, S. Tanzilli, W. Tittel, H. Zbinden, and N. Gisin, e-print quant-ph/0203067.

[13] W. Tittel, J. Brendel, H. Zbinden, and N. Gisin, Phys. Rev. Lett. **84**, 4737 (2000).

[14] G. Ribordy, J. Brendel, J.-D. Gautier, N. Gisin, and H. Zbinden, Phys. Rev. A **63**, 012309 (2001).

[15] J.D. Franson, Phys. Rev. Lett. **62**, 2205 (1989).

[16] J.F. Clauser, M.A. Horne, A. Shimony, and R.A. Holt, Phys. Rev. Lett. **23**, 880 (1969).

[17] The main reason why we use a bulk interferometer is to avoid high chromatic dispersion at 710 nm in optical fibers.

[18] G. Ribordy, J-D. Gautier, N. Gisin, O. Guinnard, and H. Zbinden, Electron. Lett. **34**, 2116 (1998).

[19] H. Zbinden, J-D. Gautier, N. Gisin, B. Huttner, A. Muller, and W. Tittel, Electron. Lett. **33**, 586 (1997).

[20] D. Stucki, G. Ribordy, A. Stefanov, and H. Zbinden, J. Mod. Opt. **48**, 1967 (2001).

[21] Note that the spectral filtering of one entangled photon also filters its twin photon.

[22] To affirm that we violate Bell inequalities, we have to make the (reasonable) assumption that the other (not recorded) triple coincidences have the same behavior, and that all coincidence count rates depend only on the sum of the phases.

[23] Y.H. Kim, M.V. Chekhova, S.P. Kulik, M.H. Rubin, and Y. Shih, Phys. Rev. A **63**, 062301 (2001).

[24] V. Scarani, A. Acin, N. Gisin, H. de Riedmatten, I. Marcikic, and H. Zbinden (unpublished).

[25] C. Santori, D. Fattal, M. Pelton, G.S. Solomon, and Y. Yamamoto, e-print cond-mat/0111242.

[26] The estimation of Alice's coupling ratio and transmission t_A is made by assuming that it is comparable to that of Bob (t_B), which can be measured knowing the coincidence count rate, the count rate of the Ge detector, and the quantum efficiency of InGaAs APD.